

IHTC16-23736

ENHANCED WATER EVAPORATION WITH FLOATING SYNTHETIC LEAVES

Weiwei Shi, Joshua R. Vieitez, Austin S. Berrier, Matthew W. Roseveare, Jonathan B. Boreyko*

Department of Biomedical Engineering and Mechanics, Virginia Tech, Blacksburg, VA 24060, USA

ABSTRACT

The evaporation of water exposed to a subsaturated environment is relevant for a variety of water harvesting and energy harvesting applications. Here, we show that the diffusive evaporation rate of water can be greatly modulated by floating a nanoporous synthetic leaf at the water's free interface. The floating leaf was able to evaporate at least as much water as a free interface under equivalent conditions, which is remarkable considering that only about a third of the leaf's interface is open to the ambient. We attribute the enhanced evaporation of the water menisci to their sharp curvature and three-dimensional surface area. At low humidities the water menisci cannot achieve a local equilibrium, due to the mismatch in water activity across the interface outcompeting the negative Laplace pressure. As a result, the mensici retreat partway into the leaf, which increases the local humidity directly above the menisci until equilibrium is reached. Using a ceramic disk with pore diameters of 160 nm, we find the surprising result that leaves exposed to an ambient relative humidity of 95% can evaporate water at the same rate as leaves exposed to only 50% humidity, due to the long and tortuous vapor pathway in the latter case.

KEY WORDS: Boiling and evaporation, porous media, synthetic tree, negative pressure, diffusion

1. INTRODUCTION

Evaporation is relevant to a variety of natural and engineered systems including transpiration, perspiration, humidification, water desalination, and vapor chambers [1–5]. In nature, trees evaporate water from their nanoporous leaves to spontaneously generate the pressure head required to lift water up the trunk [6, 6–9]. The enabling mechanism is the concave liquid-air menisci present at the evaporating interface, which generates a highly negative Laplace pressure ($P_{\text{leaf}} \approx -6 \,\text{MPa}$) that is extended down the xylem to the roots [9–11] (Figure 1). This cohesion theory of sap ascent has been known for over a century [12], yet only in the past decade have nanofabrication and microfluidic techniques advanced to the point where researchers can engineer sophisticated artificial leaf or even trees with controlled architectures [9]. The notion of using a synthetic leaf to spontaneously generate large pressure heads is still in its infancy; work so far has mostly focused on basic proof-of-concepts of synthetic trees [13, 14] or characterizing boiling instabilities [13, 15–21].

The proof-of-concept of a synthetic tree, where pure water pumps continuously from a reservoir into a transpiring "leaf", was pioneered in 1895 by Dixon and Joly, who attached porous cups to both ends of a tube [12]. In 2008, Wheeler and Stroock used modern microfabrication techniques to embed conductive micro-channels within a nanoporous hydrogel [13]; this is the first example of a sophisticated artificial tree and has inspired several follow-up tree/leaf mimics in the intervening years[14–21]. Interestingly, stable negative pressures as

*Corresponding Jonathan B. Boreyko: boreyko@vt.edu

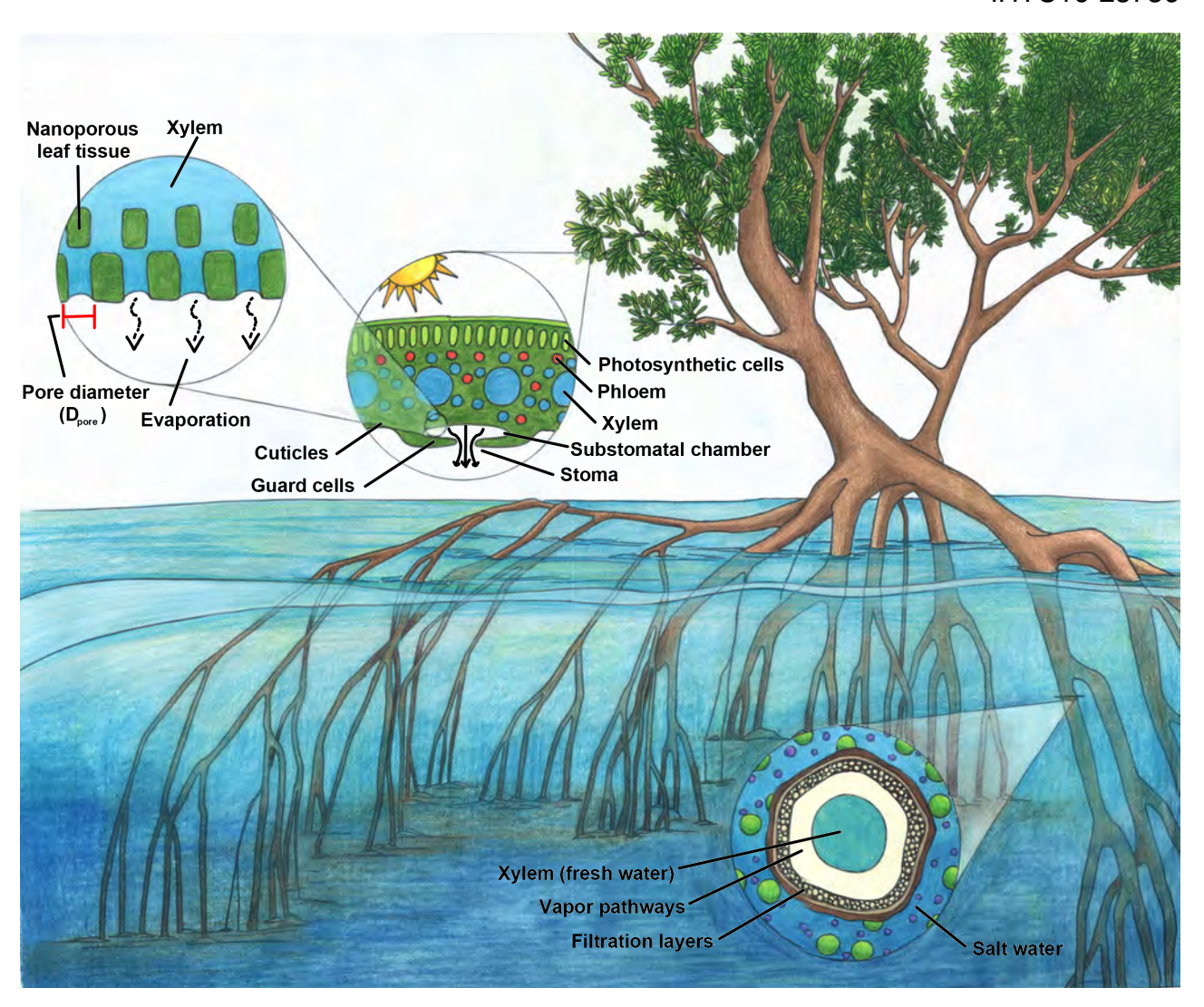


Fig. 1 Working principles of a mangrove tree. Water evaporating from nanoporous leaf tissue into a subsaturated environment generates concave water menisci with a negative pressure differential across the water-air interface (left inset). This water vapor initially concentrates in substomatal cavities and diffuses into the ambient via stomata (middle inset). The negative water pressure extends all the way down to the roots of the tree, enabling the reverse osmosis of salt water during water intake (right inset).

high as $P_{\text{leaf}} \approx -30 \, \text{MPa}$ have been measured when simplifying from a tree system (atmospheric reservoir connected to leaf) to an equivalent leaf-only system (finite water built directly inside of leaf); it is currently unclear why the stability of water flowing through a tree is more fragile than water within a stand-alone leaf [13].

In these reports, stable water was typically only possible for ambient humidities of over $90\,\%$ for synthetic trees [13] or for humidities over $80\,\%$ for synthetic leaves [20], in obvious contrast to natural trees which can survive even in very dry conditions. Finally, while the mass flux of water flowing through a "xylem" to a transpiring leaf was as high as $Q = 7 \times 10^4 \, \text{g/m}^2 \text{s}$ when heating the leaf to $60\,^{\circ}\text{C}$, water flow was across a single micro-channel ($A \approx 2 \times 10^{-10} \, \text{m}^2$), such that the maximum flow rate was only $\dot{m} = 15 \times 10^{-6} \, \text{g/s}$ [13]. Finally, an understanding of the evaporation rates of water from synthetic leaves have not been greatly explored, with many recent examples confining the "leaf" nanopores against a glass roof for purely one-dimensional evaporation about the edge of the nanoporous film [19, 20, 22].

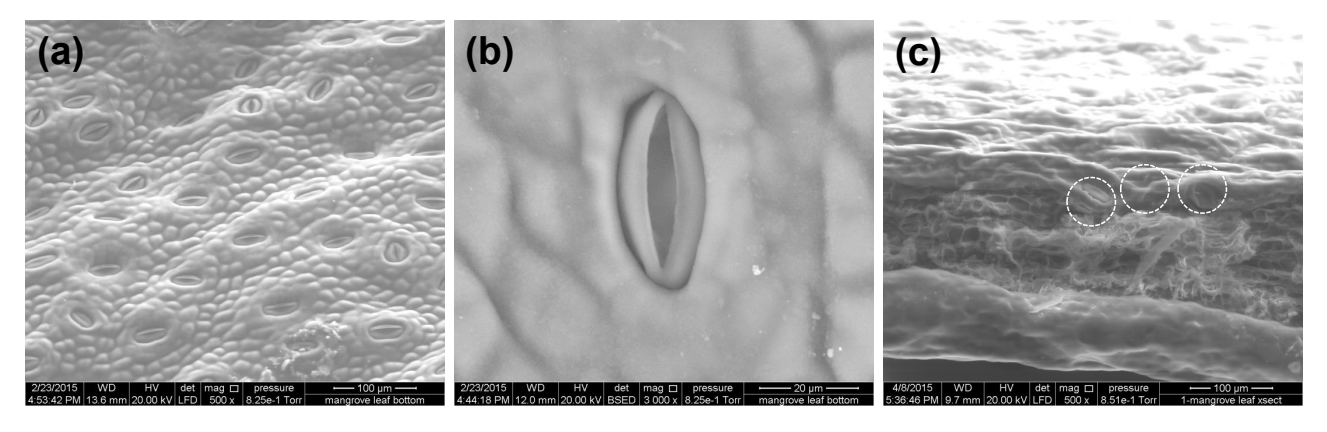


Fig. 2 (a,b) Stomatal apertures on the leaf of a red mangrove plant; (c) Red mangrove leaf with stomata (white circles) on only the abaxial side.

Here, we characterize the diffusive evaporation of water from macroscopic synthetic leaves. We focus on the three aforementioned constrains of recent reports of synthetic trees/leaves. First, we design synthetic stoma and substomatal chambers, in an attempt to locally increase the humidity and stability above the water mensici for low ambient humidities. Second, we float a large macroscopic leaf at the free interface of a water reservoir, in order to maximize the throughput of water and decouple the system from issues related to hydraulic conductance up xylem conduits. Finally, we systematically measure the evaporation rate of water from the synthetic leaves for a variety of humidities and water temperatures. Surprisingly, we find that synthetic leaves are capable of evaporating at least as much water as equivalent bulk interfaces, and are also self-stabilizing at low humidities even without the stomata. These findings suggest that synthetic leaves may be desirable for enhancing evaporation for thermal desalination or other systems.

2. EXPERIMENT AND RESULTS

To create a proof-of-concept synthetic leaf, we first characterized the morphology of natural leaves from Florida Coastal Mangroves (*Rhizophora mangle*). Mangrove saplings were washed with water and kept at the free surface of a salt water aquarium by using pieces of foam and twist ties. By adding the proper amount of Instant Ocean Sea Salt into the aquarium, the salinity and magnesium levels of the water were maintained at 21 ppt and 1,300 ppm, respectively, which corresponds to the levels of the mangroves' natural Floridian habitat.

On days where imaging was performed, samples were gently plucked from the healthiest mangrove plants. An environmental scanning electron microscope (FEI Quanta 600 FEG) at Virginia Tech's Nanoscale Characterization and Fabrication Laboratory was used to image the topology of the leaves (Figure 2). Of particular interest was characterizing the topology of the stomata. The stomata were only on the abaxial side of each leaf. Across all species, the stomatal apertures were observed to be almost exactly 30 μ m in length with average center-to-center spacings of approximately 150 μ m between adjacent stomata. The profile of the stomatal apertures was in the shape of a convex lens with a maximal width of about 10–20 μ m, although it is well known that this width varies in nature as a response to environmental conditions [23]. Also, note that these stomatal apertures were slightly recessed with respect to the surrounding cuticles on the leaf surface; such depressions are known as stomatal crypts [24]. The topography of the substomatal chambers were more difficult to visualize, even when looking at cross-sections, but chambers appeared to exhibit a depth and width of about 60 μ m each, in reasonable agreement with other reports [25, 26].

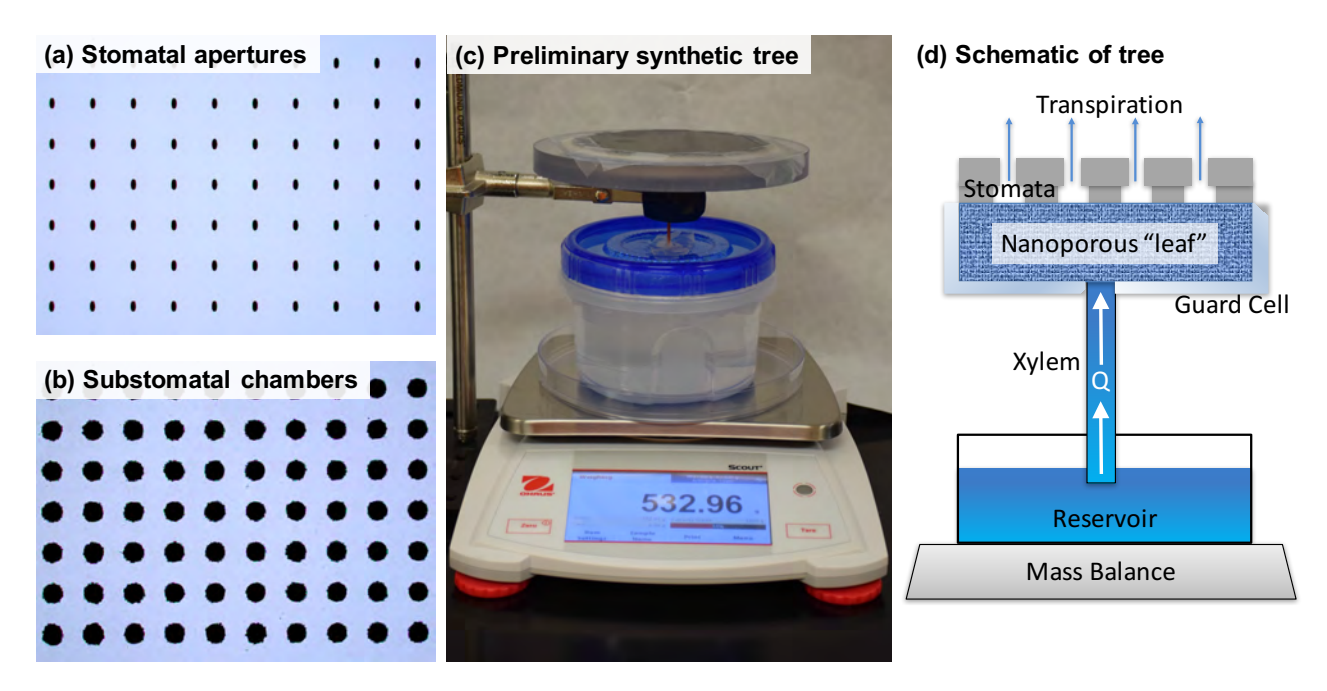


Fig. 3 (a) Fabricated stomatal apertures etched in silicon (30 μ m length, 10 μ m width, 150 μ m pitch). (b) Substomatal apertures (60 μ m diameter, 150 μ m pitch) that are aligned directly underneath the apertures. (c,d) Photo and schematic of preliminary artificial tree used here as a proof-of-concept.

2.1 Preliminary Artificial Tree

Inspired by the characterization of the mangrove leaves, a proof-of-concept of synthetic substomatal chambers and stomatal apertures were microfabricated in a cleanroom (Figure 3a,b). Using standard photolithographic techniques, arrays of substomatal chamber and arrays of stomatal apertures were microfabricated by Bosch etching all the way through 100 μ m thick silicon wafers (4 in. diameter) patterned with photoresist. For the substomatal chambers, each chamber exhibited a cross-sectional diameter of 60 μ m and arrays of chambers were organized in a square lattice configuration with the center-to-center pitch between chambers being 150 μ m. For wafers containing the stomatal apertures, the length of each aperture was 30 μ m while the maximum convex width was set to 20 μ m to mimic the varying shapes of natural stomata. Alignment marks were placed on each wafer, so that pairs of wafers could be easily oriented to align the substomatal chambers directly beneath the stomata. To approximate the leaf tissue, porous ceramic disks with an average pore size of $D_{\rm pore} \approx 160$ nm (105 mm diameter and 6.4 mm thick) were bought from Soilmoisture Equipment [14]. To mimic a xylem, high-pressure PEEK tubing (127 μ m inner diameter, 1.59 mm outer diameter) was attached to each ceramic disk by drilling a small cavity into the center of the disk's back face, inserting one end of the tube, and sealing with a water-tight silicone adhesive.

Before each experiment, the synthetic leaf (i.e. ceramic disk) and xylem (tube) were vigorously boiled in a pot of water for at least an hour to degas the water inside of the leaf and xylem. Immediately after boiling was complete, the free end of the xylem was inserted into a plastic container (this was done underwater to fill the container with the degassed water). The synthetic tree system was then removed from the large pot; the reservoir (i.e. filled plastic container) was placed on top of a mass balance interfaced with a computer. The synthetic leaf was elevated in the air above the reservoir, such that the free end of the xylem tube terminates inside of the underlying water reservoir (Figure 3c,d). For trials that include the synthetic stomata (i.e. silicon wafers), the leaf was placed in a polycarbonate "guard cell" that closed off the bottom face and side walls of the disk, such that water could only transpire from the top face out of the stomata. Parafilm was used to seal the gap between the wafers and the polycarbonate guard cell, to ensure that all vapor must flow through the substomatal chambers and out the stomatal apertures. The mass of the water traveling from the reservoir, up

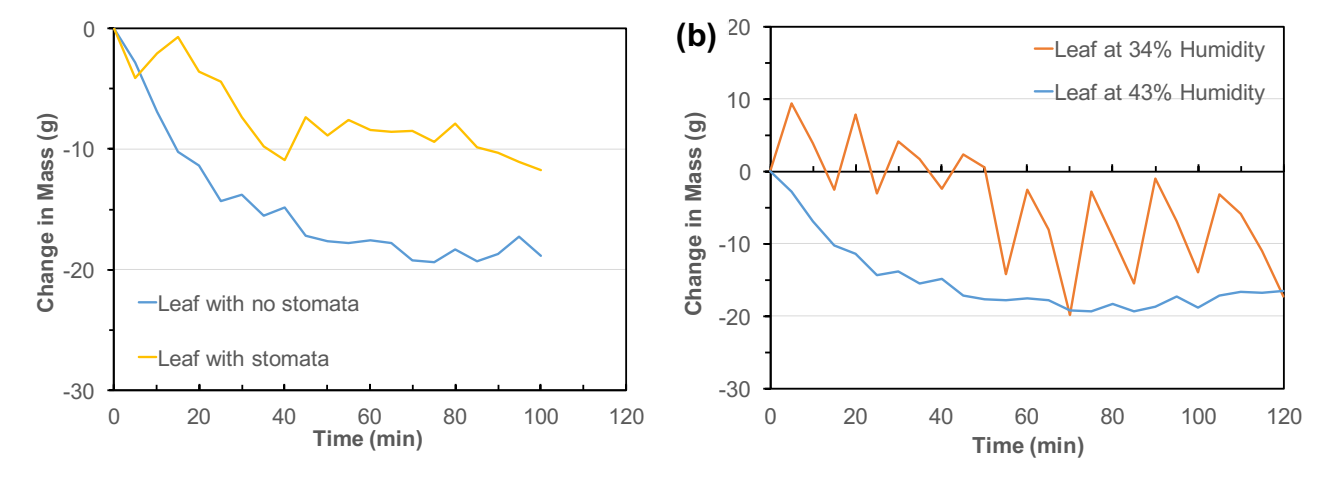


Fig. 4 The change in mass of water in a reservoir over time due to flow up the attached synthetic tree. (a) The transpiration rate of water through a tree, both with (yellow) and without (blue) stomata, with an ambient humidity of about 50%. The pore size in the leaf is $D_{\text{pore}} = 160 \text{ nm}$. (b) The same tree with bare leaves (no stomata) exhibited relatively stable transpiration for about 30 min. when exposed to 43% ambient humidity, but very noisy behavior (i.e. boiling/dryout) at a lower humidity (34%).

the xylem, and into the transpiring leaf was measured over time to gauge the stability and throughput of water in the synthetic tree.

The preliminary results of our rudimentary synthetic tree are presented in Figure 4. Encouragingly, water was able to continuously flow up the tube and into the leaf, indicating that the synthetic tree is both transpiring and acting as a hydraulic pump. While not directly visible, this transpiration is directly evident from the decrease in mass of the water reservoir over time. While slightly less robust, our synthetic tree was similarly able to pump water from the reservoir when the guard cell, substomatal chambers, and stomatal apertures were added to the synthetic leaf. To ensure that these positive results were not simply due to bulk evaporation of the water reservoir out of its container, a control experiment was performed without a xylem inserted into the reservoir, where it was seen that the loss in mass over time was completely negligible. However, it can be seen that the transpiration process only lasted for about 30 min, followed by some type of dryout instability.

One possibility is that the dryout is being caused by the low humidity ($\approx 50\%$) of the ambient. The importance of controlling the humidity becomes apparent when considering the Kelvin equation:

$$P_{\text{leaf}} = P_{\text{air}} + \frac{RT}{\nu_{\text{liq}}} \ln \left(a_{\text{vap}} \right) \tag{1}$$

where $P_{\rm air}=1$ atm, R is the ideal gas constant, T is the temperature, $v_{\rm liq}$ is the molar volume of liquid water, and $a_{\rm vap}=P_{\rm vap}/P_{\rm sat}={\rm RH}/100$ is the activity of the water vapor directly above the leaf. The Kelvin equation shows that the mismatched water activity between the (saturated) liquid water in the leaf and the (subsaturated) water vapor in the ambient requires the leaf's water to drop to a lower pressure than the ambient pressure in order for the water menisci to remain in physical equilibrium [13]. Even a relative humidity of RH=90% ($a_{\rm vap}=0.9$) yields a negative leaf pressure of $P_{\rm leaf}<-10\,{\rm MPa}$, hence the repeated observation that cavitation and/or dryout instabilities tend to occur when RH<85% ($a_{\rm vap}=0.85$) [13]. Therefore a careful control over the ambient humidity is crucial.

Another way of thinking about this is that the ambient humidity prescribes the negative pressure needed by the leaf's water to obtain equilibrium, and this value is physically obtained by the water-air menisci assuming the proper concave curvature. This can be seen quantitatively by considering the relationship between the maximum possible negative water pressure in the leaf and its pore size:

$$P_{\text{leaf}} = P_{\text{air}} - \Delta P_{max} = 1 \text{ atm} - \frac{2\sigma\cos\theta}{r_{pore}}$$
(2)

where $P_{\rm air}=1$ atm is the atmospheric air pressure, ΔP_{max} is the maximum possible pressure differential across the water-air menisci interfaces in the leave's pores (Laplace equation), $\cos\theta$ is the intrinsic contact angle of water with the leaf surface, and r_{pore} is the average radius of the pores in the leaf. Regarding the maximum possible hydraulic load itself, water in an external reservoir getting drawn by the roots will exhibit an atmospheric pressure, such that:

$$\Delta P_{\text{load}} = 1 \text{ atm} - |P_{\text{leaf}}| = \frac{2\sigma\cos\theta}{r_{\text{pore}}}$$
 (3)

For the case of the porous ceramic leaf, $\theta \approx 0^{\circ}$ and $r_{pore} = 80 \, \text{nm}$, such that $\Delta P_{\text{load}} \approx 1.8 \, \text{MPa}$ is the highest possible hydraulic load that the synthetic tree can sustain. When comparing to the Kelvin equation, this would seemingly mandate a critical humidity of 99% beyond which the menisci are not physically stable.

Another possibility is that the dryout is simply caused by the poor conductance of water up the single tube relative to the large size of our leaf. According to Darcy's law, the viscosity of the fluid and the pressure drop over a given distance through the porous leaf is:

$$\Delta P_{\text{leaf}} = \frac{Qd\mu}{\kappa A} \tag{4}$$

where Q is the volumetric flow rate, d is the thickness of the leaf (6.4 mm), μ is the viscosity of water, $\kappa = 2.0 \times 10^{-13}$ is the intrinsic permeability of the leaf, and A is the cross-sectional area of the xylem tubing (with $R_{\text{xylem}} = 63.5 \, \mu\text{m}$). Applying the equation to the data in Figure 4b, with the mass balance measurements of $Q = 2.40 \times 10^{-9} \, \text{m}^3/\text{s}$ at 34% humidity and $Q = 8.15 \times 10^{-10} \, \text{m}^3/\text{s}$ at 43%, the pressure drop within the leaf is about $\Delta P_{\text{leaf}} = 5.34 \times 10^6 \, \text{Pa}$ and $1.81 \times 10^6 \, \text{Pa}$, respectively. The lower humidity, the higher the flowrate and pressure drop. For the pressure drop in the xylem, the Poiseuille equation can be applied:

$$\Delta P_{\text{xylem}} = \frac{8QL\mu}{\pi R_{\text{xylem}}^4} \tag{5}$$

where L=0.061 m is the length of the xylem tubing and Q is the same measured values as before. The pressure drop across the tubing is estimated to be 2.04×10^4 Pa and 6.93×10^3 Pa, respectively, for the 34% and 43% humidities. This is 2–3 orders of magnitude larger than the pressure drop across the leaf itself, which confirms that the xylem conduit is severely restricting the throughput of water across the tree.

2.2 Floating Leaf

Hypothesizing that the poor conductance of the xylem was to blame for the rapid dryout of our synthetic tree, we now switch to a "floating leaf" setup where the bottom half of the leaf is in direct contact with the water reservoir (Figure 5a). In this manner, we can isolate the effects of humidity on the stability of the leaf, without additionally having to consider the hydraulic conductance issues of the xylem. The PVC reservoir (McMaster Carr) was filled with degassed (i.e. boiled) water and the ceramic disc ($D_{\rm pore} = 160~\rm nm$) was seated in the polycarbonate guard cell which contained a large hole in its bottom to allow for the intake of water. To securely float the leaf at the free interface of the reservoir, polyethylene foam was secured around the edge of the guard cell, taking care to minimize the gap between the foam and the wall of the PVC reservoir. In this manner, the vast majority of the water evaporation had to occur through the leaf, not from the edges of the reservoir. As before, the stomatal layers were optionally placed atop the leaf for some experiments. In another control case, the PVC reservoir was simply filled with degassed water but with no leaf on top at all, to gauge the evaporation rate of an equivalent surface area but without the influence of the nanopores. As the water was still warm from the boiling process, the temperature of water within the reservoir was measured with a data logger. The ambient humidity of the air was set using a large humidity chamber that enclosed the setup (Electro-Tech Systems, Inc.).

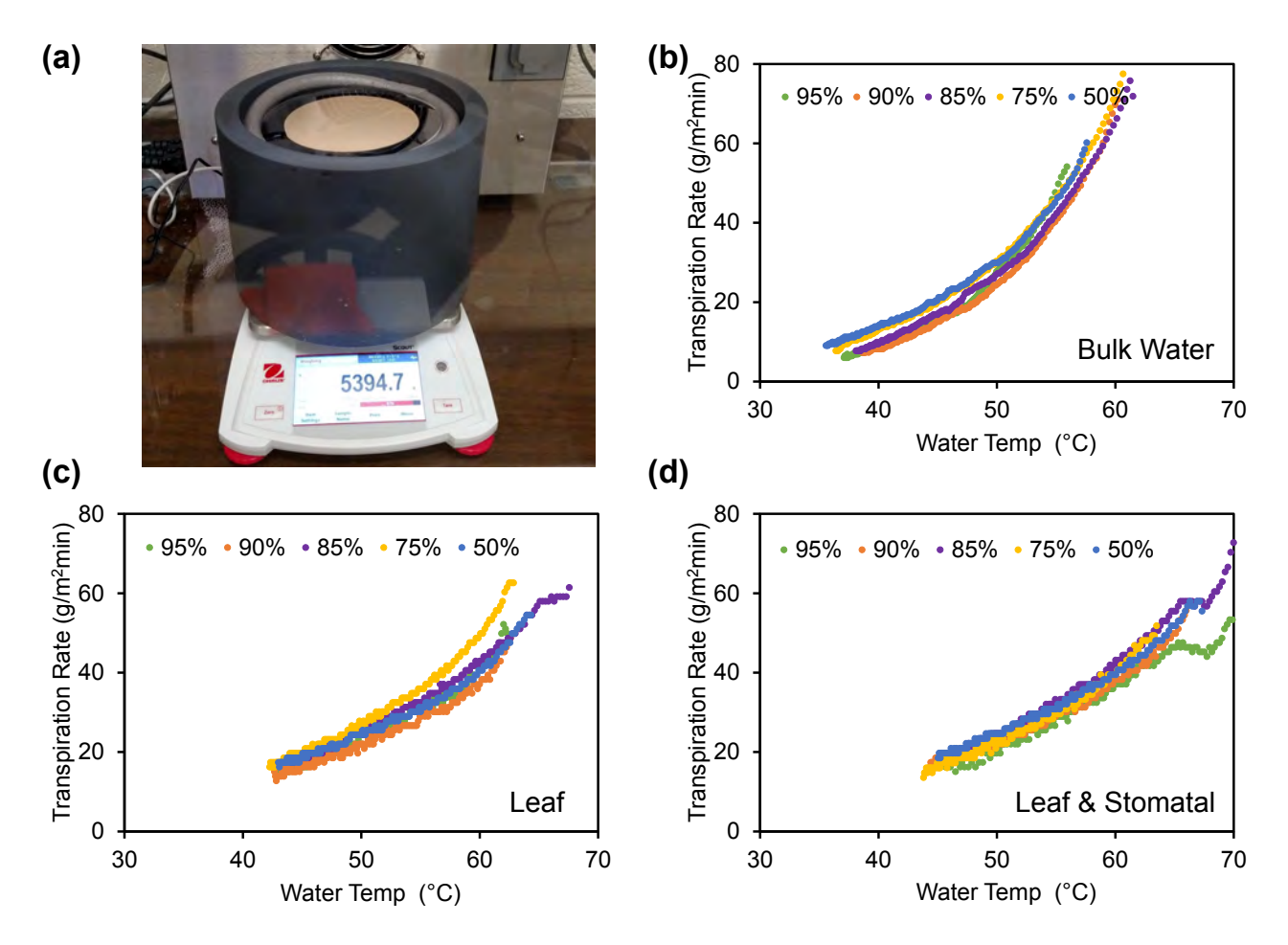


Fig. 5 (a) The setup of floating leaf without silicon stomata. (b-d) The transpiration rate under five different humidities for (b) bulk water, (c) a bare floating leaf, and (d) a floating leaf overlaid with silicon stomata.

First, the diffusive evaporation rate of bulk water was obtained (Figure 5b) with chamber humidities of 50%, 75%, 85%, 90%, or 95%. As expected, for the bulk water the evaporation rate increased with decreasing humidity. Traditionally, in terms of evaporation, the Fick's law of diffusion governs the transport:

$$Q_{\text{evap}} = -D_{\text{f}} \frac{\partial C}{\partial x} \tag{6}$$

where Q_{evap} is the mass flux, C is the vapor concentration, x is the position and D_f is the binary diffusion coefficient of the air-vapor mixture. Based off Fick's law, the lower humidity, the lower vapor concentration, the higher evaporation rate.

For the floating leaf setup, the pressure drop inside the "tree" is just generated by the porous leaf. According to Darcy's Law (Equation 4), the pressure drop inside the leaf is $12.8 \, \text{Pa}$, $11.7 \, \text{Pa}$, $15.5 \, \text{Pa}$, $14.6 \, \text{Pa}$, $13.6 \, \text{Pa}$, for 95%, 90%, 85%,75% and 50%, respectively, which are far smaller than the maximum Laplace pressure $(1.8 \times 10^6 \, \text{Pa})$ of the curvature:

$$\Delta P_{\text{leaf}} = \frac{Qd\mu}{\kappa A} \ll \Delta P_{max} \tag{7}$$

Where $Q_{\rm evap} \approx Q$. The evaporation rate from the leaf determines the Laplace pressure it needs, rather than the flow rate from the reservoir to the leaf. It demonstrated that the porous leaf produced the dominant pressure which lift the water from the reservoir, balanced with a smaller Laplace pressure. Thus the Laplace pressure is much smaller than the maximum one.

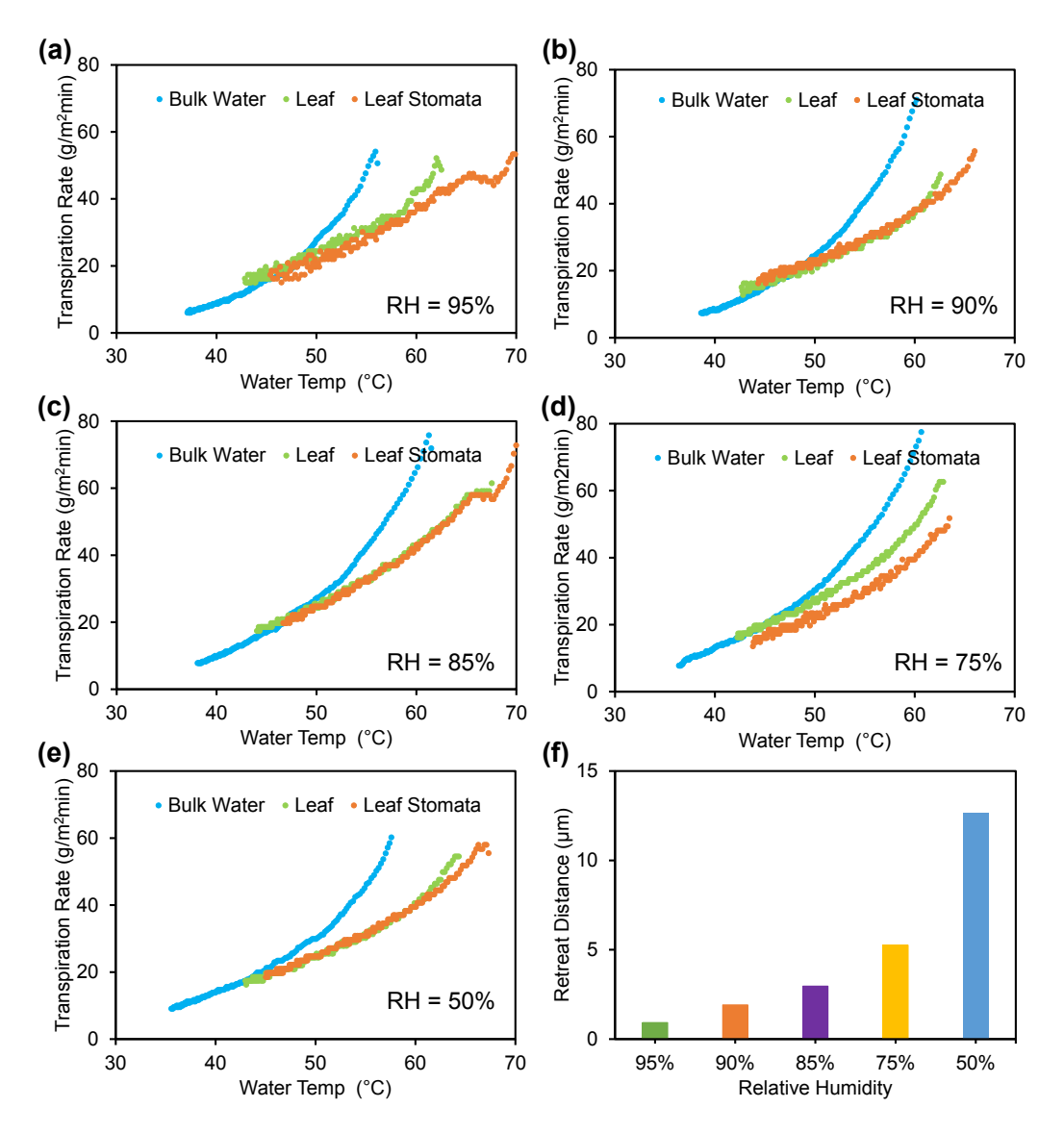


Fig. 6 Comparison among bulk water, floating leaf and leaf with stomata. (a) 95% (b) 90% (c) 85% (d) 75% (e) 50%. (f) Model quantifying the critical receding distance of menisci within the nanopores until self-stabilizing for a given ambient humidity.

Encouragingly, the evaporation rate for the floating leaf setup was extremely stable over several hours, in contrast with the dryout instability of the full tree setup. But surprisingly, the evaporation rate of water within the floating leaf was not increasing monotonically with decreasing humidity (Figure 5c), in seeming contradiction with Fick's law. For example, the leaf exposed to an ambient relative humidity of 95% can evaporate water at the same rate as leaves exposed to only 50% humidity. Furthermore, the evaporation rates for 75% and 85% humidities were actually higher than for 50%! Adding the stomata atop the leaf did not change the results greatly (Figure 5d), but did slightly reshuffle which humidities exhibited higher evaporation rates than others. For example, the 85% humidity exhibited the highest evaporation rate with the stomata, compared to 75% for the bare leaf.

The two surprising aspects of evaporation from a floating leaf: the stability at low humidities and the non-monotonic dependence on humidity, can simultaneously be explained as follows. Recall from the Kelvin and Laplace equations that for our given pore size, the menisci should become physically unstable and retreat beneath a critical humidity of 99%. However, as the menisci retreat by some distance l, the evaporative vapor

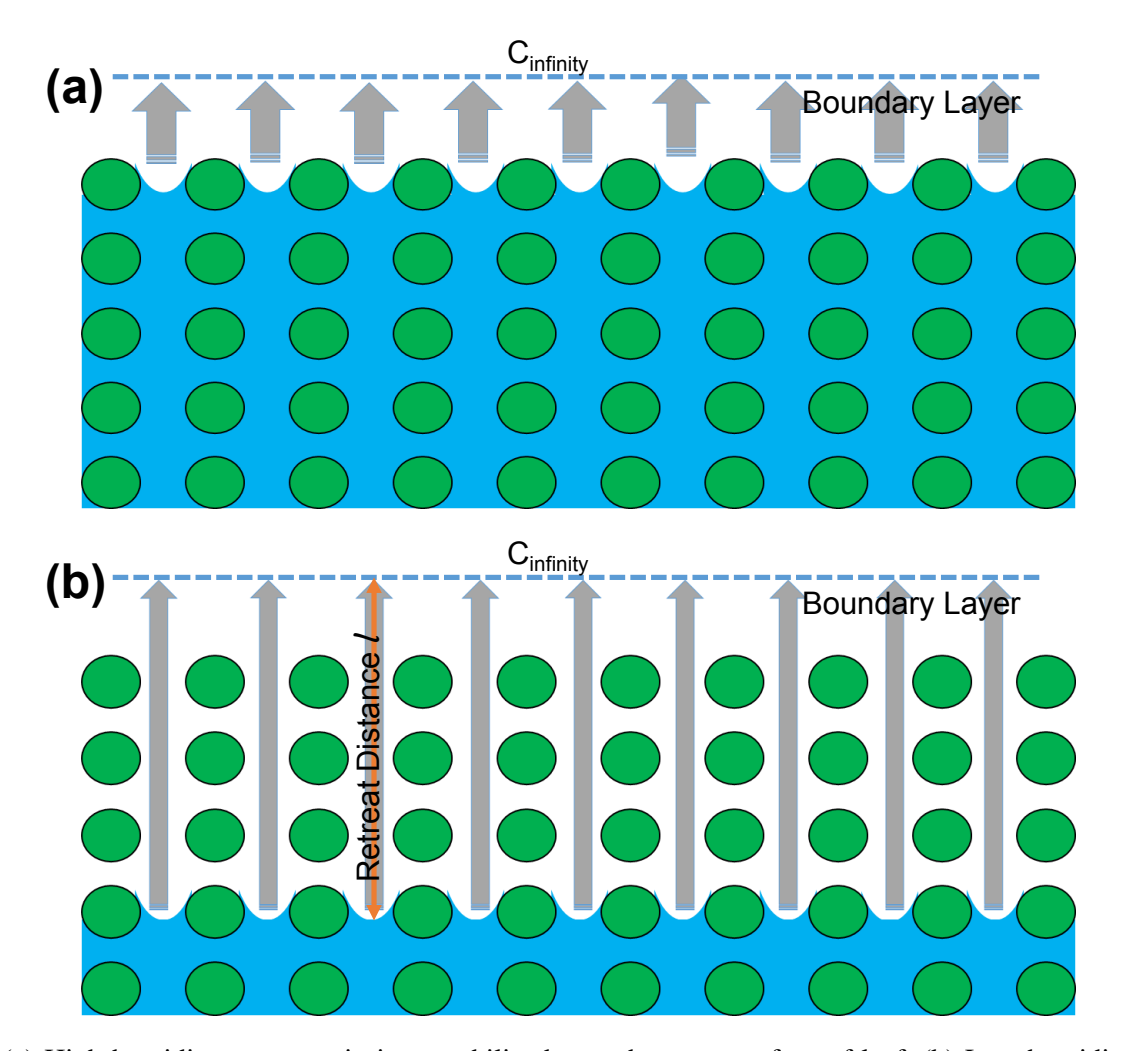


Fig. 7 (a) High humidity case: menisci are stabilized near the outer surface of leaf. (b) Low humidity case: Menisci have to partially retreat within leaf to find equilibrium.

becomes choked within the nanoporous media thus increasing the local humidity to a higher value. Eventually, the retreating menisci will self-stabilize after reaching a critical l where the local humidity now corresponds to the critical value. In this steady-state situation, it has recently been modeled by Stroock et al. that the critical retreat length l is given by [22]:

$$\frac{l}{d-l} = \frac{P_c - P_{ext}}{-P_c} \times \beta \tag{8}$$

where P_c is the capillary pressure, deduced from Eqns 3 and 4 and P_{ext} is the external pressure, deduced from Eqn 1. The ratio of conductances $\beta = g_{vap}/g_{liq}$, which is estimated as 2.125×10^{-6} for our pore size $r_{pore} = 80$ nm. g_{liq} is the linear mass conductivity of a liquid-filled pore and g_{vap} the linear mass conductivity of a vapor-filled pore. Applying the evaporation rate of the floating leaf in Figure 5c into Eqn 8, the retreat distance is l = 0.93 μ m, 1.92 μ m, 2.96 μ m, 5.26 μ m and 12.67 μ m respectively with decreasing humidity (Figure 6f). As expected, with lower humidity, the retreat distance is longer.

This calculation explains both mysteries at once. First, it reveals that for sufficiently thick porous media, the menisci can be self-sustained even at low ambient humidities by simply retreating partway within the porous media. In other words, the stomata do not seem necessary purely from a water cycle standpoint, particularly given their challenges in fabricating. Second, it explains the non-monotonic dependence of the evaporation rate on the ambient humidity. At high ambient humidities, the menisci stabilize closer to the outer interface of

the leaf's nanopores, which has the benefit of minimizing the concentration boundary layer but the detriment of decreasing the gradient in vapor concentration. At lower ambient humidities, the concentration gradient is now maximal, but so is the boundary layer. Thus, both extremes have their tradeoffs, explaining why water evaporates at the same rate within the leaf for 95% and 50% humidities.

3. CONCLUSIONS

In conclusion, by floating a nanoporous leaf at the free interface of bulk water, the diffusive evaporation rate can be dramatically modified. Using a ceramic disk with pore diameters of 160 nm, leaves exposed to an ambient relative humidity of 95 % can evaporate water at the same rate as leaves exposed to only 50 % humidity, due to the long and tortuous vapor pathway in the latter case caused by the retreating menisci. It is remarkable that the evaporation rates from the leaves were commensurate with those from an equivalent free interface, given that only 1/3 of the leaf's interface was comprised of water menisci. We attribute this to the concave curvature of the menisci, as it is well known that evaporation is enhanced with both curvature and increased interfacial surface area. Finally, we note that the synthetic stomata added to the leaf were proven unnecessary, as the nanopores of the leaf itself were sufficient to self-stabilize the water menisici when exposed to low humidities. We expect that by adding further functionality, such as using thermally absorptive materials, that floating synthetic leaves can be useful for enhancing thermal evaporation.

ACKNOWLEDGMENTS

This work was supported by a National Science Foundation CAREER Award (CBET-1653631). The microfabrication of the synthetic stomata was conducted at the Center for Nanophase Materials Sciences (CNMS) at the Oak Ridge National Laboratory as a user project (User Project CNMS2015-R48). We gratefully acknowledge technical assistance with the cleanroom microfabrication at CNMS from Patrick Collier and Bernadeta Srijanto.

REFERENCES

- [1] H. H. Mosher. Simultaneous study of constituents of urine and perspiration. J. Biol. Chem., 99:781–790, 1933.
- [2] Z. Lu, K. L. Wilke, D. J. Preston, I. Kinefuchi, E. Chang-Davidson, and E. N. Wang. An ultrathin nanoporous membrane evaporator. *Nano Lett.*, 17:6217–6220, 2017.
- [3] Z. Lu, T. R. Salamon, S. Narayanan, K. R. Bagnall, D. F. Hanks, D. S. Antao, B. Barabadi, J. Sircar, M. E. Simon, and E. N. Wang. Design and modeling of membrane-based evaporative cooling devices for thermal management of high heat fluxes. *IEEE Trans. Compon. Packag. Manuf. Technol.*, 6:1056–1065, 2016.
- [4] D. Laing, C. Bahl, T. Bauer, D. Lehmann, and W. Steinmann. Thermal energy storage for direct steam generation. *Sol. Energy*, 85:627–633, 2011.
- [5] Emad M.S. El-Said A.E. Kabeel. A hybrid solar desalination system of air humidification, dehumidification and water flashing evaporation: Part ii. experimental investigation. *Desalination*, 341:5060, 2014.
- [6] P. F. Scholander. How mangroves desalinate seawater. Physiol. Plant., 21:251–261, 1968.
- [7] A. K. Parida and B. Jha. Salt tolerance mechanisms in mangroves: a review. *Trees*, 24:199–217, 2010.
- [8] K. Kim, E. Seo, S. K. Chang, T. J. Park, and S. J. Lee. Novel water filtration of saline water in the outermost layer of mangrove roots. *Sci. Rep.*, 6:20426, 2016.
- [9] A. D. Stroock, V. V. Pagay, M. A. Zwieniecki, and N. M. Holbrook. The physicochemical hydrodynamics of vascular plants. *Annu. Rev. Fluid Mech.*, 46:615–642, 2014.
- [10] G. W. Koch, S. C. Sillett, G. M. Jennings, and S. D. Davis. The limits to tree height. Nature, 428:851–854, 2004.
- [11] N. M. Holbrook and M. A. Zwieniecki. Vascular transport in plants. Academic Press, 2011.
- [12] H. H. Dixon and J. Joly. On the ascent of sap. Philos. Trans. R. Soc. B, 186:563-576, 1895.

- [13] T. D. Wheeler and A. D. Stroock. The transpiration of water at negative pressures in a synthetic tree. *Nature*, 455:208–212, 2008.
- [14] M. Lamb, G. W. Koch, E. R. Morgan, and M. W. Shafer. A synthetic leaf: the biomimetic potential of graphene oxide. *Proc. of SPIE*, 9429:1–10, 2015.
- [15] T. D. Wheeler and A. D. Stroock. Stability limit of liquid water in metstable equilibrium with subsaturated vapors. *Langmuir*, 25:7609–7622, 2009.
- [16] J. Li, C. Liu, Z. Xu, K. Zhang, X. Ke, and L. Wang. A microfluidic pump/valve inspired by xylem embolism and transpiration in plants. *PLOS ONE*, 7:e50320, 2012.
- [17] O. Vincent, P. Marmottant, P. A. Quinto-Su, and C. D. Ohl. Birth and growth of cavitation bubbles within water under tension confined in a simple synthetic tree. *Phys. Rev. Lett.*, 108:184502, 2012.
- [18] C. Duan, R. Karnik, M. C. Lu, and A. Majumdar. Evaporation-induced cavitation in nanofluidic channels. *Proc. Natl. Acad. Sci. U.S.A.*, 109:3688–3693, 2012.
- [19] O. Vincent, D. A. Sessoms, E. J. Huber, J. Guioth, and A. D. Stroock. Drying by cavitation and poroelastic relaxations in porous media with macroscopic pores connected by nanoscale throats. *Phys. Rev. Lett.*, 113:134501, 2014.
- [20] I. T. Chen, D. A. Sessoms, Z. Sherman, E. Choi, O. Vincent, and A. D. Stroock. Stability limit of water by metastable vapor-liquid equilibrium with nanoporous silicon membranes. *J. Phys. Chem. B*, 120:5209–5222, 2016.
- [21] J. M. Li, C. Liu, Z. Xu, K. P. Zhang, X. Ke, C. Y. Li, and L. D. Wang. A bio-inspired microump based on stomatal transpiration in plants. *Lab Chip*, 11:2785–2789, 2011.
- [22] O. Vincent, A. Szenicer, and A. D. Stroock. Capillarity-driven flows at the continuum limit. *Soft Matter*, 12:6656–6661, 2016.
- [23] H. Kim and S. J. Lee. Stomata-inspired membrane produced through photopolymerization patterning. *Adv. Funct. Mater.*, 25:4496–4505, 2015.
- [24] F. Hassiotou, J. R. Evans, M. Ludwig, and E. J. Veneklaas. Stomatal crypts may facilitate diffusion of co₂ to adaxial mesophyll cells in thick sclerophylls. *Plant Cell Environ.*, 32:1596–1611, 2009.
- [25] W. F. Pickard. How does the shape of the substomatal chamber affect transpirational water loss? *Math. Biosci.*, 56:111–127, 1981.
- [26] A. Roth-Nebelsick. Computer-based studies of diffusion through stomata of different architecture. Ann. Bot., 100:23–32, 2007.